Journal of Organometallic Chemistry, 370 (1989) 407–419
Elsevier Sequoia S.A., Lausanne – Printed in The Netherlands
JOM 09685

Dynamic behaviour and X-ray analysis of chiral η^3-allylpalladium complexes. II

Edoardo Cesarotti, Maria Grassi *, Laura Prati,

Università di Milano, Dipartimento di Chimica Inorganica e Metallorganica, Via Venezian 21, I-20133 Milano (Italy)

and Francesco Demartin *

Università di Milano, Istituto di Chimica Strutturistica Inorganica, Via Venezian 21, I-20133 Milano (Italy)

(Received November 21st, 1988)

Abstract

The DANTE technique and NOESY two-dimensional method have been employed to observe the isomerization of the chiral cationic complex $[Pd(\eta^3\text{-}CH_2CMeCH_2(P\text{–}P'))]^+$ (**1a**), where P–P′ = the chiral chelating ligand (*S*)(*N*-diphenylphosphino)(2-diphenylphosphinoxymethyl)pyrrolidine. The rate constant was found to be $\ll 0.5\ s^{-1}$ in $CHCl_3$ at 295 K and $1.50\ s^{-1}$ in the presence of added free ligand. In the latter case the epimerization proceeds by a π–σ–π mechanism via the intermediacy of a primary η^1-allylpalladium complex. Although the intermediate was not detected, the NMR findings reveal that it has the allylic terminus η^1-bonded to palladium. The structure of **1a** in its PF_6^- salt has been determined. The compound crystallizes in the orthorhombic space group $P2_12_12_1$ with *a* 10.029(4) *b* 19.203(8) *c* 36.115(6) Å, $Z = 8$, $R = 0.0572$ and $R_w = 0.0712$ for 3716 observed reflections with $I > 3\sigma(I)$.

Introduction

Chiral organometallic compounds have attracted considerable interest as catalysts for asymmetric carbon–carbon bond formation [1]. Among this wide range of reactions much attention has been focused on allylic alkylation catalyzed by group VIII metals [2]. It is widely accepted that in allylic alkylation catalyzed by palladium compounds the key intermediates are π-allyl-Pd(P–P′)$^+$ complexes, generated by oxidative addition of an allylic acetate to a phosphine palladium(0) species, and that the turn-over limiting step as well as the stereodifferentiating step is the attack of the nucleophile on the allyl moiety. Since the empirical applied procedures [3] are far ahead of the theoretical understanding, small variations in the

0022-328X/89/$03.50

nature of the reactants still produce unpredictable results. In the search for higher enantioselectivity we thought it of interest to establish how the stereoelectronic properties of a suitable chiral chelating ligand change the properties of allylation intermediates and products. NMR spectroscopy proved to be very valuable for this purpose, and enabled determination of the stereochemistry and the chirality in solution of the two diastereoisomeric forms of the complex $[Pd(\eta^3\text{-}C_4H_7(P\text{-}P')]^+X^-$ (**1**), (where P–P′ = the chiral chelating ligand ((*S*)(*N*-diphenylphosphino)(2-diphenylphosphinoxymethyl)pyrrolidine)) = ((*S*)-Prolophos) and $X^- = BF_4^-$, PF_6^-) and of the *trans* influence of the coordinated ligand analyzed [4]. We report here the X-ray structure and the dynamic behaviour in solution of the PF_6^- salt of complex **1** in optically pure form.

Results and discussion

The ligand and complex **1** were prepared and fully characterized as previously reported [4,5]. Complex **1** exists in solution in two diastereoisomeric forms **1a** and **1b**, in equilibrium ratio ($CHCl_3$, 295 K) **1a**/**1b** = 2.5/1; their structures were assigned on the basis of NMR data. Slow recrystallization of the diastereomeric mixture from methanol gave crystals of pure **1a** ($X^- = PF_6^-$) suitable for an X-ray diffraction study.

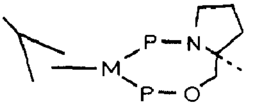

(1a)

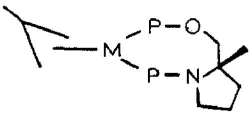

(1b)

Description of the structure

Crystals of **1a** consist of $[Pd(\eta^3\text{-}C_4H_7)((S)\text{-Prolophos-P-P}')]^+$ cations and PF_6^- anions, with the packing determined by van der Waals interactions. The shortest contact between cations and anions is F(4)...H(112), 2.46 Å. The asymmetric unit consists of two independent PF_6^- anions and two $[Pd(\eta^3\text{-}C_4H_7)((S)\text{-Prolophos})\text{-P-P}')]^+$ cations. The atomic coordinates for the refined model are reported in Table 1. Selected bond distances, angles and torsion angles are shown in Table 2. The main differences between the two cations essentially relate to the conformation of the phenyl rings of the ligand ((*S*)-Prolophos) which lie in an approximately axial position with respect to the P–Pd–P plane. For molecule 1 the C(121)–C(126) and C(221)–C(226) planes are essentially perpendicular to each other (dihedral angle of 91°), whereas in molecule 2 the corresponding C(321)–C(326) and C(421)–C(426) planes are almost parallel (14°). Small differences are observed in the conformational parameters of the seven-membered rings (see Table 2), which, in both molecules are in the boat-type conformation, with the oxygen atom lying in the coordination plane. Such a conformation of the ((*S*)-Prolophos) moiety has been observed in all the previously reported complexes containing this diphosphine ligand [5,6], which under the influence of packing requirements, can more readily adjust, by rearrangement of the conformation of the phenyl groups, than can the rest of the molecule. Although the essential features of the two cations are clear, the molecular parameters are somewhat affected by high e.s.d.'s. The final difference

Table 1

Fractional atomic coordinates for non-hydrogen atoms

Atom	x	y	z
Pd(1)	0.7333(1)	0.80295(6)	0.71420(3)
P(1)	0.9512(4)	0.7806(2)	0.7300(1)
P(2)	0.6844(4)	0.6961(2)	0.6904(1)
O(11)	0.806(1)	0.6404(5)	0.6878(3)
N(31)	1.031(1)	0.7386(6)	0.6979(3)
C(11)	0.913(2)	0.6492(8)	0.6615(4)
C(21)	0.973(2)	0.7192(8)	0.6611(4)
C(41)	1.181(2)	0.739(1)	0.6954(5)
C(51)	1.206(2)	0.730(1)	0.6554(6)
C(61)	1.080(2)	0.7212(9)	0.6339(4)
C(71)	0.719(2)	0.9085(8)	0.7348(4)
C(81)	0.591(2)	0.8772(9)	0.7387(5)
C(91)	0.542(2)	0.851(1)	0.7039(5)
C(101)	0.534(2)	0.861(1)	0.7756(5)
C(111)	1.050(2)	0.8592(8)	0.7404(4)
C(112)	1.047(2)	0.9062(9)	0.7121(5)
C(113)	1.124(2)	0.971(1)	0.7193(6)
C(114)	1.179(2)	0.982(1)	0.7504(6)
C(115)	1.184(2)	0.932(1)	0.7775(6)
C(116)	1.115(2)	0.8676(9)	0.7740(5)
C(121)	0.965(2)	0.7274(7)	0.7719(4)
C(122)	0.911(2)	0.7553(9)	0.8041(5)
C(123)	0.916(2)	0.715(1)	0.8380(6)
C(124)	0.980(2)	0.653(1)	0.8357(5)
C(125)	1.028(2)	0.631(1)	0.8057(5)
C(126)	1.034(2)	0.6674(8)	0.7720(4)
C(211)	0.603(1)	0.6938(7)	0.6460(3)
C(212)	0.594(1)	0.7531(7)	0.6255(4)
C(213)	0.538(2)	0.7540(8)	0.5905(4)
C(214)	0.477(2)	0.6942(8)	0.5782(4)
C(215)	0.486(2)	0.6353(8)	0.5968(4)
C(216)	0.543(2)	0.6351(8)	0.6306(4)
C(221)	0.578(1)	0.6537(7)	0.7239(4)
C(222)	0.461(2)	0.6197(8)	0.7183(4)
C(223)	0.392(2)	0.588(1)	0.7465(5)
C(224)	0.431(2)	0.5944(9)	0.7808(5)
C(225)	0.549(2)	0.625(1)	0.7872(6)
C(226)	0.618(2)	0.655(1)	0.7605(6)
Pd(2)	0.9756(1)	0.96169(6)	0.00872(3)
P(3)	1.1046(4)	0.9144(2)	0.0550(1)
P(4)	1.1314(4)	1.0414(2)	−0.0082(1)
O(12)	1.250(1)	1.0538(5)	0.0206(2)
N(32)	1.153(1)	0.9741(6)	0.0847(3)
C(12)	1.226(2)	1.0850(7)	0.0566(4)
C(22)	1.126(1)	1.0471(7)	0.0799(4)
C(42)	1.200(2)	0.9612(8)	0.1236(4)
C(52)	1.117(2)	1.015(1)	0.1445(5)
C(62)	1.127(2)	1.0795(8)	0.1195(4)
C(72)	0.809(2)	0.8918(9)	0.0175(4)
C(82)	0.807(2)	0.907(1)	−0.0216(6)
C(92)	0.798(3)	0.986(1)	−0.0269(6)
C(102)	0.844(3)	0.860(1)	−0.0538(7)
C(311)	1.032(2)	0.8435(7)	0.0842(4)
C(312)	0.916(2)	0.8598(8)	0.1005(4)

Table 1 (continued)

Atom	x	y	z
C(313)	0.853(2)	0.809(1)	0.1245(5)
C(314)	0.922(2)	0.745(1)	0.1283(5)
C(315)	1.027(2)	0.7316(8)	0.1121(4)
C(316)	1.091(2)	0.7808(7)	0.0883(4)
C(321)	1.241(1)	0.8731(7)	0.0359(4)
C(322)	1.236(2)	0.8388(8)	0.0012(4)
C(323)	1.345(2)	0.8079(9)	−0.0169(4)
C(324)	1.469(2)	0.8115(9)	0.0037(5)
C(325)	1.482(2)	0.8425(9)	0.0354(5)
C(326)	1.377(2)	0.8770(8)	0.0520(4)
C(411)	1.073(1)	1.1282(7)	−0.0203(4)
C(412)	0.957(2)	1.1525(8)	−0.0081(4)
C(413)	0.924(2)	1.2203(9)	−0.0151(5)
C(414)	0.995(2)	1.2659(8)	−0.0355(4)
C(415)	1.112(2)	1.2404(9)	−0.0481(5)
C(416)	1.158(2)	1.1731(8)	−0.0416(4)
C(421)	1.234(2)	1.0114(7)	−0.0461(4)
C(422)	1.354(2)	0.9883(7)	−0.0430(4)
C(423)	1.420(2)	0.962(1)	−0.0731(5)
C(424)	1.358(2)	0.953(1)	−0.1061(5)
C(425)	1.230(2)	0.974(1)	−0.1118(5)
C(426)	1.163(2)	1.0046(9)	−0.0816(5)
P(10)	0.2837(5)	0.5245(3)	0.1496(1)
P(11)	0.6557(5)	1.0496(3)	0.1065(2)
F(1)	0.146(1)	0.5113(9)	0.1675(4)
F(2)	0.223(1)	0.554(1)	0.1156(3)
F(3)	0.281(2)	0.4581(9)	0.1281(6)
F(4)	0.291(2)	0.5911(6)	0.1677(5)
F(5)	0.410(1)	0.535(1)	0.1313(4)
F(6)	0.346(2)	0.489(1)	0.1832(4)
F(7)	0.642(2)	0.9767(7)	0.0946(5)
F(8)	0.525(2)	1.037(1)	0.1280(6)
F(9)	0.588(2)	1.0763(9)	0.0717(5)
F(10)	0.781(2)	1.059(2)	0.0879(5)
F(11)	0.666(2)	1.1165(7)	0.1276(5)
F(12)	0.703(2)	1.022(1)	0.1412(4)

Fourier map revealed residual peaks, especially in the region of the allyl moiety of molecule 2, and these may be attributable to a small degree of disorder, which is also reflected in high thermal parameters for the refined atoms and precludes a more detailed discussion.

NMR results

Formula A shows the labelling of the ^{31}P and ^{1}H resonances and the primes (′) denote the signals of the corresponding minor isomer. The isomerization of **1a**

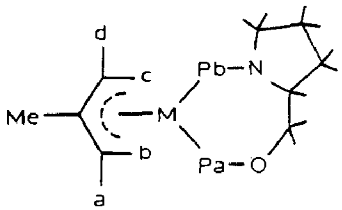

Table 2

Selected bond distances (Å), angles (deg.) and torsion angles (deg.) with e.s.d.'s in parentheses for complex **1a**

(a) Distances (Å)			
Pd(1)-P(1)	2.299(3)	Pd(2)-P(3)	2.302(3)
Pd(1)-P(2)	2.278(3)	Pd(2)-P(4)	2.272(3)
Pd(1)-C(71)	2.16(1)	Pd(2)-C(72)	2.16(1)
Pd(1)-C(81)	2.20(1)	Pd(2)-C(82)	2.28(2)
Pd(1)-C(91)	2.17(1)	Pd(2)-C(92)	2.25(2)
P(1)-N(31)	1.624(8)	P(3)-N(32)	1.642(8)
N(31)-C(21)	1.50(1)	N(32)-C(22)	1.44(1)
C(21)-C(11)	1.47(1)	C(22)-C(12)	1.50(1)
C(11)-O(11)	1.44(1)	C(12)-O(12)	1.45(1)
O(11)-P(2)	1.623(7)	O(12)-P(4)	1.595(7)
N(31)-C(41)	1.51(2)	N(32)-C(42)	1.50(1)
C(41)-C(51)	1.47(2)	C(42)-C(52)	1.53(2)
C(51)-C(61)	1.50(2)	C(52)-C(62)	1.53(2)
C(61)-C(21)	1.45(1)	C(62)-C(22)	1.56(1)
P(1)-C(111)	1.84(1)	P(3)-C(311)	1.87(1)
P(1)-C(121)	1.83(1)	P(3)-C(321)	1.73(1)
P(2)-C(211)	1.80(1)	P(4)-C(411)	1.82(1)
P(2)-C(221)	1.81(1)	P(4)-C(421)	1.81(1)
C(71)-C(81)	1.43(2)	C(72)-C(82)	1.44(2)
C(81)-C(91)	1.44(2)	C(82)-C(92)	1.54(2)
C(81)-C(101)	1.49(2)	C(82)-C(102)	1.52(2)
P(10)-F(1,6) average	1.486	P(11)-F(7,12) average	1.485
Bond angles (deg.)			
P(1)-Pd(1)-P(2)	97.5(1)	P(3)-Pd(2)-P(4)	94.3(1)
Pd(1)-P(1)-N(31)	112.4(3)	Pd(2)-P(3)-N(32)	111.3(3)
P(1)-N(31)-C(21)	124.5(7)	P(3)-N(32)-C(22)	123.3(6)
N(31)-C(21)-C(11)	112.2(9)	N(32)-C(22)-C(12)	114.5(8)
C(21)-C(11)-O(11)	114.6(9)	C(22)-C(12)-O(12)	114.3(8)
C(11)-O(11)-P(2)	121.2(6)	C(12)-O(12)-P(4)	121.7(6)
O(11)-P(2)-Pd(1)	117.0(3)	O(12)-P(4)-Pd(2)	115.8(3)
C(21)-N(31)-C(41)	109.7(9)	C(22)-N(32)-C(42)	109.3(8)
N(31)-C(41)-C(51)	103.(1)	N(32)-C(42)-C(52)	100.2(9)
C(41)-C(51)-C(61)	112.(1)	C(42)-C(52)-C(62)	103.(1)
C(51)-C(61)-C(21)	106.(1)	C(52)-C(62)-C(22)	102.6(9)
C(61)-C(21)-N(31)	108.0(9)	C(62)-C(22)-N(32)	106.2(8)
C(11)-C(21)-C(61)	109.3(6)	C(12)-C(22)-C(62)	108.5(8)
C(71)-C(81)-C(91)	112.(1)	C(72)-C(82)-C(92)	109.(1)
C(91)-C(81)-C(101)	122.(1)	C(92)-C(82)-C(102)	129.(1)
C(71)-C(81)-C(101)	125.(1)	C(72)-C(82)-C(102)	120.(1)
(b) Torsion angles (deg.) within the seven-membered rings			
Pd(1)-P(1)-N(31)-C(21)	2.9	Pd(2)-P(3)-N(32)-C(22)	−4.9
P(1)-N(31)-C(21)-C(11)	−92.5	P(3)-N(32)-C(22)-C(12)	−85.7
N(31)-C(21)-C(11)-O(11)	59.9	N(32)-C(22)-C(12)-O(12)	53.2
C(21)-C(11)-O(11)-P(2)	48.9	C(22)-C(12)-O(12)-P(4)	57.2
C(11)-O(11)-P(2)-Pd(1)	−70.7	C(12)-O(12)-P(4)-Pd(2)	−66.7
O(11)-P(2)-Pd(1)-P(1)	−4.6	O(12)-P(4)-Pd(2)-P(3)	−15.2
P(2)-Pd(1)-P(1)-N(31)	43.7	P(4)-Pd(2)-P(3)-N(32)	55.6

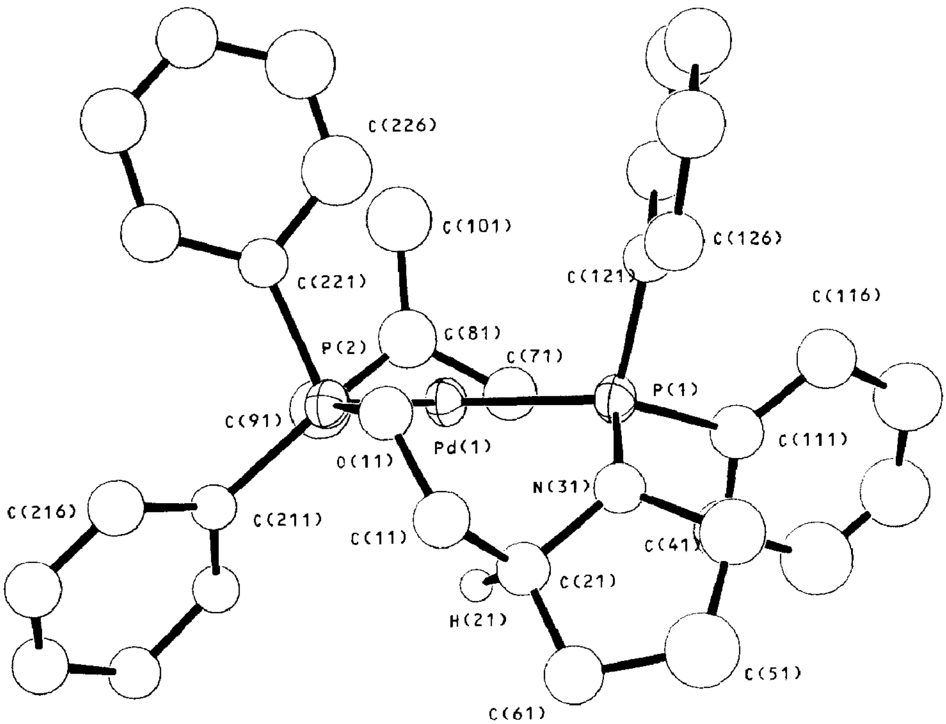

Fig. 1. ORTEP drawing for complex **1a** (first independent molecule); thermal ellipsoids are drawn at 30% probability.

(shown in eq. 1) can be readily monitored by ^{31}P NMR spectroscopy (Fig. 3).

$$\mathbf{1a} \rightleftharpoons \mathbf{1b} \qquad (1)$$

When **1a** was dissolved in $CDCl_3$ at 213 K, the ^{31}P spectrum revealed the presence of only a trace of **1b**. When the temperature was raised, a progressive increase of the signals of the second isomer occurred, and at 295 K the spectrum of the thermodynamic mixture was observed; it consists of two sets of doublets: δ 72.9 (Pb), 122.2 (Pa) for **1a** and δ 74.0 (Pb′), 124.8 (Pa′) for **1b**. NMR spectroscopy is very powerful in qualitative and quantitative investigation of dynamic processes [7]. Since no averaging of chemical shifts and couplings was observed in the ^{31}P and ^{1}H spectra of **1** at 295 K we conclude that under the conditions used the isomers **1a** and **1b** are undergoing slow exchange (i.e. they appear static on the NMR time scale). Providing that the exchange rate is not slower than the relaxation rate of the examined spin system, slow processes can be monitored by 2D- and 1D-exchange spectroscopy [9,10]. On the basis of the negative results of both 2D-^{1}H and 2D-^{31}P chemical exchange spectra and ^{31}P magnetization transfer measurements on **1** ($CDCl_3$, 295 K), T_1 being 1.6 s and 2.0 s for Pa and Pb, respectively, the rate constant for the exchange shown in eq. 1 must be $\ll 0.5\ s^{-1}$. Isomerization of **1** occurs more rapidly on addition of a trace of ((*S*)-Prolophos). Although the ^{31}P spectrum of **1** under these conditions remained unchanged and no signals from the free ligands or new species were detected, a DANTE spin saturation transfer experiment [10] on this sample provided evidence for a dynamic process. The higher field line of Pa was excited, and transfer to the corresponding line of Pa′ was

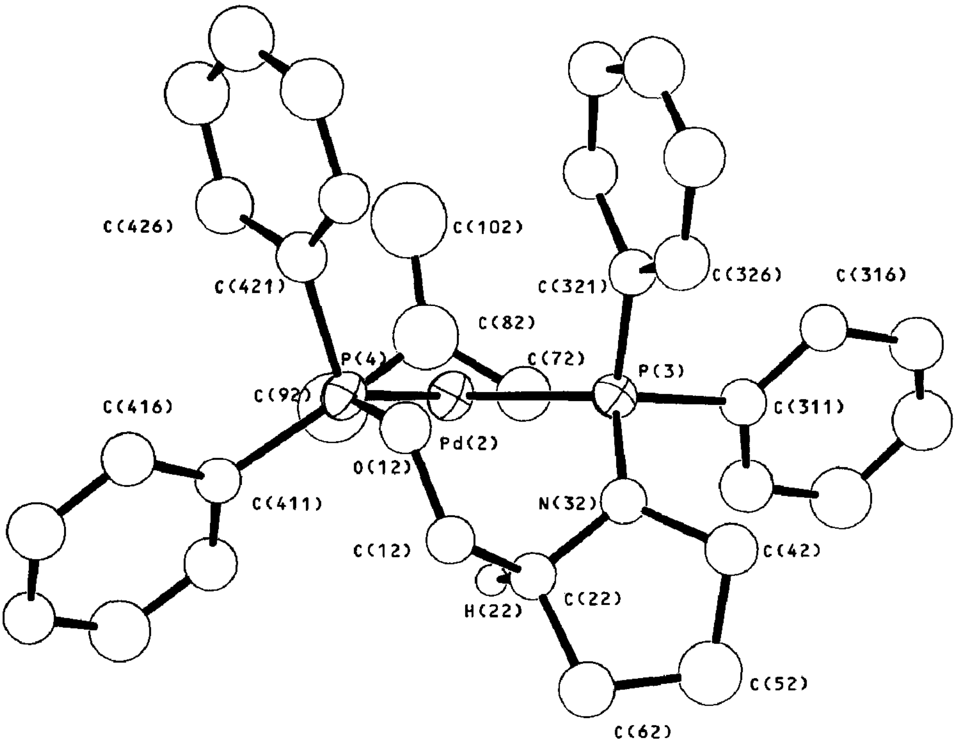

Fig. 2. ORTEP drawing for complex **1a** (second independent molecule); thermal ellipsoids are drawn at 30% probability.

observed (Fig. 4). These findings indicate that the exchange represented by eq. 1 is now occurring on a time detectable by the NMR method. Analysis of the data (Fig. 5) shows that the isomerization rate constant for 1 in the presence of added

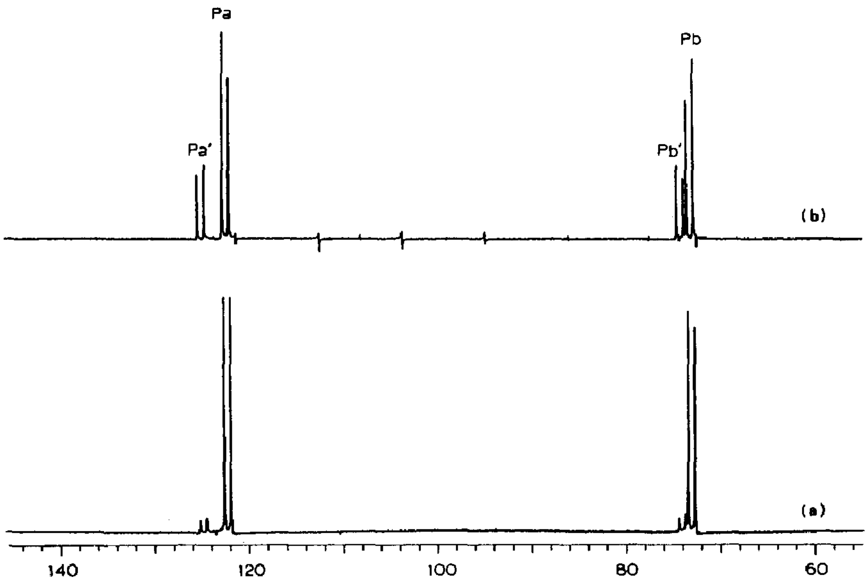

Fig. 3. $^{31}P\{^1H\}$ (81.015 MHz, $CDCl_3$) spectrum for complex **1**: (a) at 213 K, (b) at 295 K.

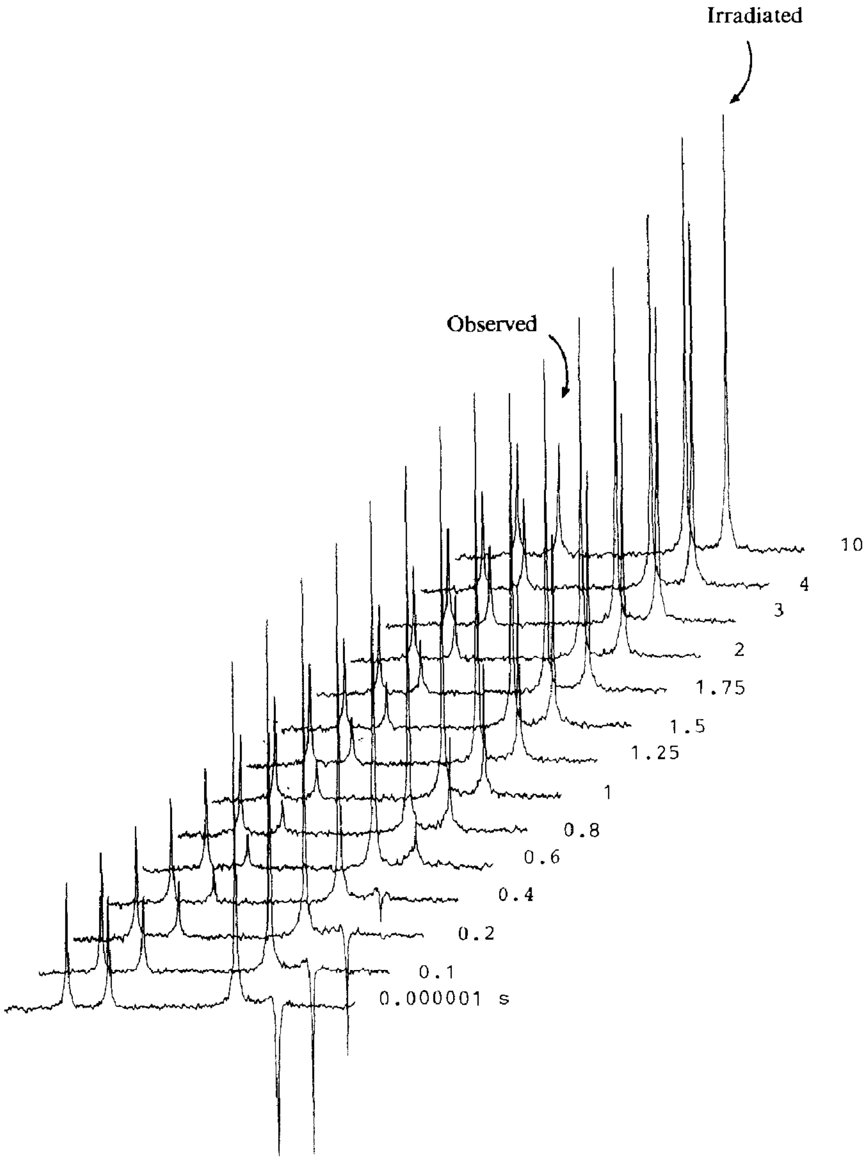

Fig. 4. Intramolecular magnetization transfer in complex **1** (81.015 MHz, $CDCl_3$, 295 K) in the presence of added (*S*)-Prolophos with irradiation of the higher field line of Pa by a DANTE sequence. Each spectrum was accumulated after the delay shown after the selective inversion. Note that the signal from the exchanging site (higher field line of Pa′) initially decreases in intensity, which is followed by a return to equilibrium magnetization.

((*S*)-Prolophos) is 1.50 s^{-1} in $CHCl_3$ at 295 K. Addition of a substantial excess of ((*S*)-Prolophos) caused the appearance in the ^{31}P spectrum of the signals of the free ligand as broad singlets at δ 114.0 (PO) and δ 46.4 (PN). A DANTE spin saturation transfer procedure was carried out with this sample. Irradiation of the PN resonance at δ 46.4 led to excitation transfer to 72.9 (Pb). Accordingly the ^{31}P 2D-chemical exchange spectrum shows exchange between both arms of free and coordinated ((*S*)-Prolophos) (Fig. 6), thus suggesting that the isomerization of **1** involves

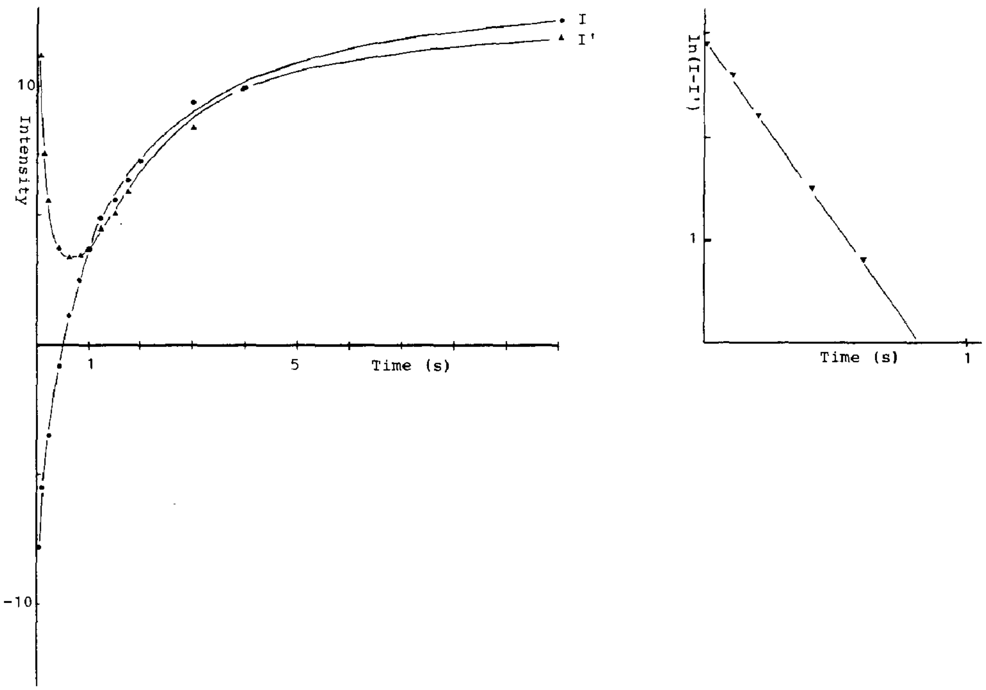

Fig. 5. Results of an inversion transfer experiment. The intensities I and I' of Pa and Pa′ are shown as a function of the delay after inversion of Pa. The intensity values of Pa′ have been multiplied by $K = 2.5$ in order to equalize the population of the two exchanging sites. The gradient of the plot of $\ln(I - I')$ against time gave a rate constant of $1.50\ s^{-1}$ for the epimerization of **1** in $CDCl_3$, 295 K, $T_1(Pa) = 1.6$ s.

participation of the free ligand. These observations are readily accounted for if it is assumed that complex **1** isomerizes by a π–σ–π mechanism [11] involving the intermediacy of an η^1-allylpalladium complex that could not be detected in the ^{31}P spectrum (Scheme 1). Since the η^1–η^3 isomerization should lead to equilibration of the *syn* and *anti* protons on the allyl carbon η^1-bonded to palladium, a clear answer can be obtained by ^1H NMR spectroscopy. A phase sensitive NOESY [12] spectrum was recorded for **1** in the presence of added ((*S*)-Prolophos), and two cross sections of the counter plot are shown in Fig. 7. (In this methodology no ambiguity exists in the 2D spectrum, the resonances due to chemical exchange being opposite in sign with respect to those due to positive proton proton NOE's). Analysis of the results shows that there is intermolecular chemical exchange between the following paris of allylic protons: a, b′; b, a′; c, c′ and d, d′. These findings mean that the NMR

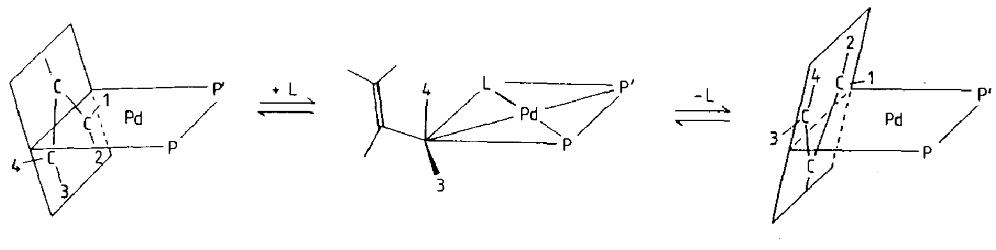

Scheme 1. The mechanism of *syn*–*anti* interchange for complex **1**.

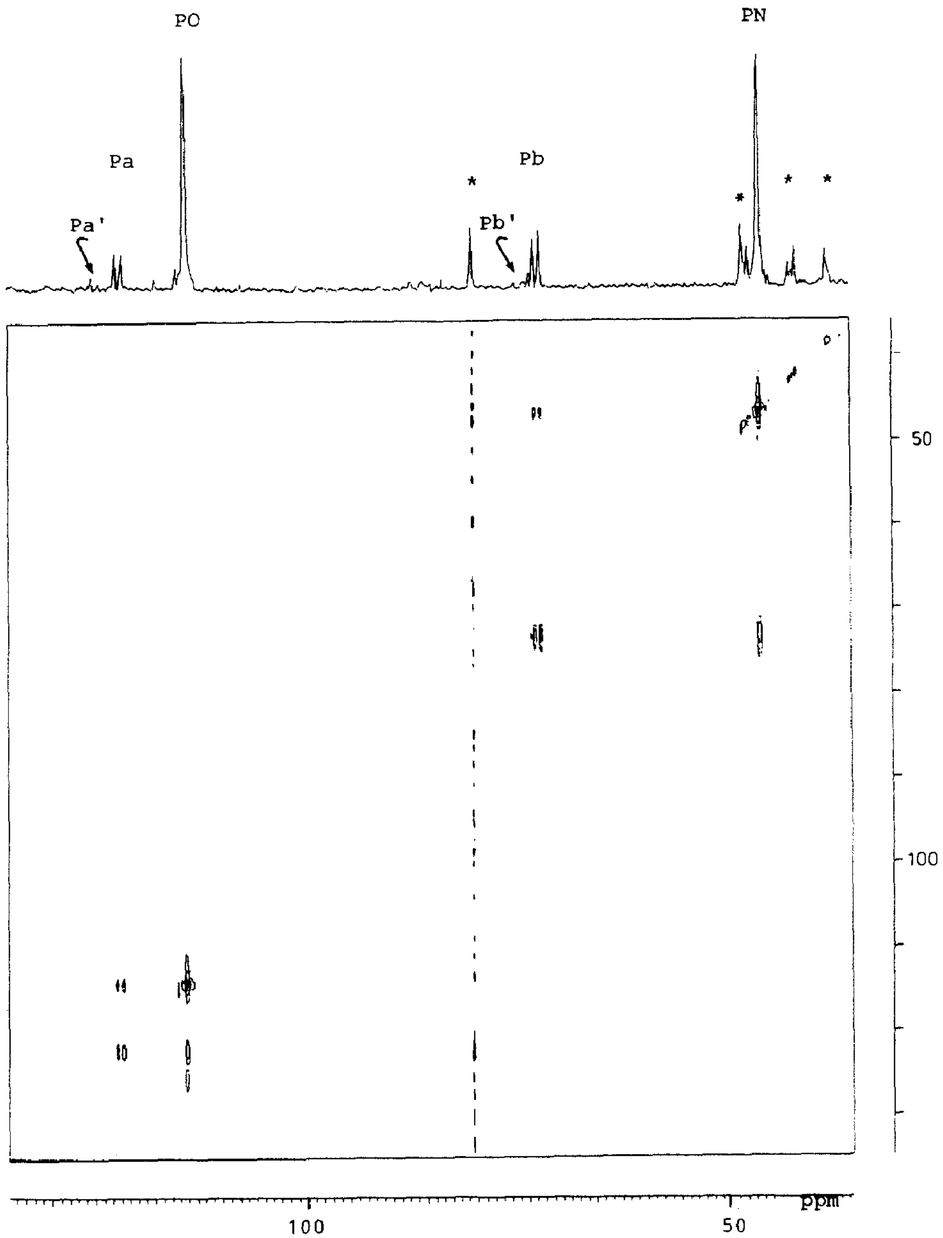

Fig. 6. Counter plot of the ^{31}P exchange spectrum (NOESY sequence) of **1** (81.015 MHz, $CDCl_3$, 295 K) in the presence of added (*S*)-Prolophos. The diagonal and a few cross peaks of **1b** are under the threshold of the plot.

detectable isomerization of **1** proceeds by a $\pi-\sigma-\pi$ mechanism involving formation of an η^1-allylpalladium intermediate exclusively at the allylic carbon opposite to PN.

Conclusion

An X-ray diffraction study of complex **1a** has confirmed the stereochemistry assignment based on NMR findings [4]. Dynamic NMR measurements indicate that

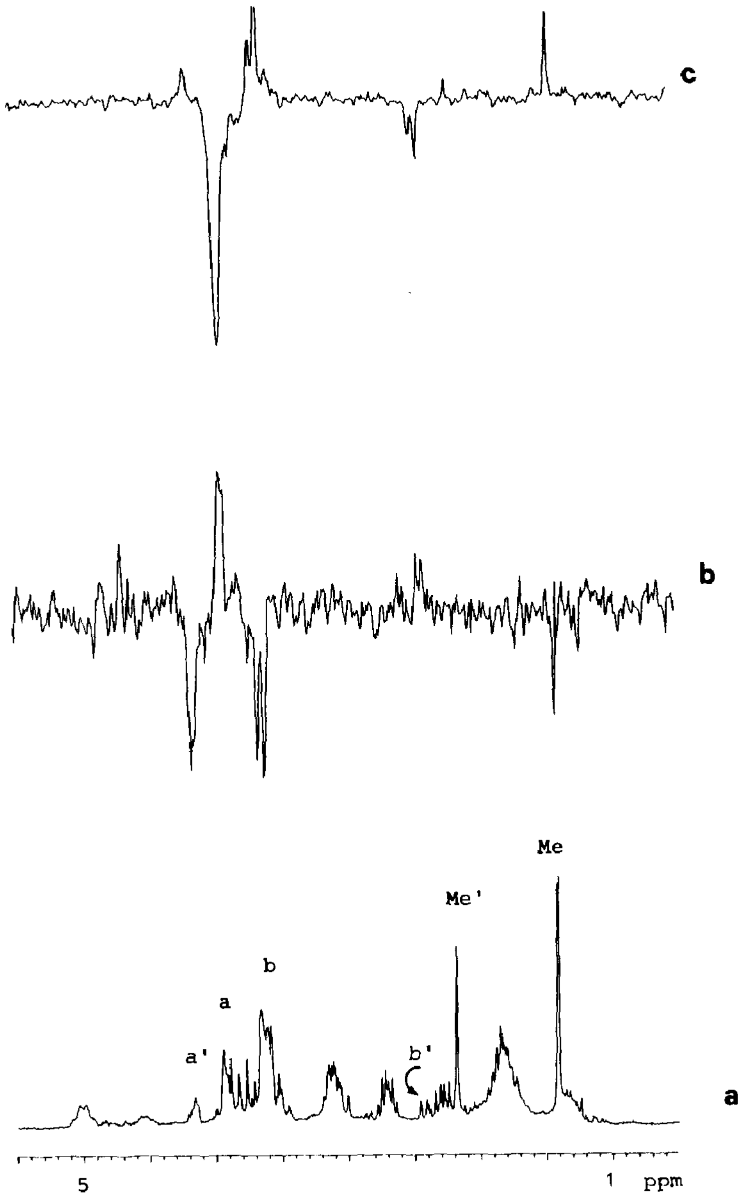

Fig. 7. (a) Aliphatic region of the ^{1}H spectrum of 1 (200.13 MHz, $CDCl_3$, 295 K) (b) and (c): cross section of the ^{1}H exchange spectrum (NOESY phase sensitive sequence) of 1 (200.13 MHz, $CDCl_3$, 295 K) in the presence of added (*S*)-Prolophos. Negative and positive absorptions indicate exchange and proton NOE's, respectively, (b) shows exchange between the protons b and a′; (c) shows exchange between the protons a and b′.

this complex readily isomerizes by a π–σ–π mechanism involving formation of an η^1-allylpalladium bond exclusively at the allylic carbon opposite to PN.

Experimental

Complex **1** was prepared by a published method [4]. The NMR spectra were recorded on Bruker AC-200 and Varian XL-200 spectrometers. Magnetization

Table 3

Crystallographic data

Formula	$C_{33}H_{29}F_6NOP_3Pd$
F.w. (amu)	1537.84
Crystal system	orthorhombic
Space group	$P2_12_12_1$
a (Å)	10.029(4)
b (Å)	19.203(8)
c (Å)	36.115(6)
U (Å^3)	6955(7)
Z	8
$D_{calc.d}$ (g cm^{-3})	1.469
μ(Mo-K_α) (cm^{-1})	7.19
Min. transmission factor	0.97
Crystal dimensions (mm)	0.12×0.10×0.18
Scan mode	ω
ω-scan width (°)	1.3+0.35 tan θ
θ-range (°)	3–25
Octants of reciprocal space explored	$+h$, $+k$, $+l$
Measured reflections	6786
Unique observed reflections with $I > 3\sigma(I)$	3716
Final R and R_w indices [a]	0.0572, 0.0712
No. of variables	461
ESD [b]	2.253

[a] $R = [\Sigma(F_o - k|F_c|)/\Sigma F_o]$, $R_w = [\Sigma w(F_o - k|F_o|)^2/\Sigma_w F_o^2]^{1/2}$. [b] ESD $= [\Sigma w(F_o - k|F_c|)^2/(N_{observations} - N_{variables})]^{1/2}$; $w = 1/(\sigma(F_o))^2$; $\sigma(F_o) = [\sigma^2(I) + (0.04I)^2]^{1/2}/2F_o$Lp.

transfer experiments were carried out by the DANTE pulse sequence. Typically a series of a hundred 3.2 μs pulses spaced by 0.625 ms provided a selective π pulse at the centre frequency, and was followed by a delay time, which was varied from 100 ms to 10 s before a non-selective $\pi/2$ observe pulse was applied. Values of T_1 were determined by the inversion recovery method. The NOESY spectra were obtained using standard pulse sequences [13] with a mixing time of 2 s.

X-Ray data collection and structure determination

Crystal data and other experimental details are summarized in Table 3. The diffraction experiment was carried out on an Enraf–Nonius CAD-4 diffractometer at room temperature and using Mo-K_α radiation (λ 0.71073 Å). The calculations were performed on a PDP 11/34 computer using the SDP-plus Structure Determination Package [14]. The diffracted intensities were corrected for Lorentz and polarization effects and absorption (empirical correction) [15]. Scattering factors and anomalous dispersion corrections for atomic scattering factors of non-hydrogen atoms were taken from ref. 16.

The structure was solved by conventional Patterson and Fourier methods and refined by full matrix least-squares, with minimization of the function $\Sigma w(F_o - k|F_c|)^2$. Anisotropic thermal factors were refined for Pd, P, and F atoms. Except for those of the allyl moiety, the hydrogen atoms were introduced at calculated positions, and were not refined. The choice of the correct enantiomorph was made on the basis of previous knowledge of the absolute configuration of C(21) and C(22) in the proline moiety. Nevertheless the refinement of the other enantiomer was tested, and yielded only slightly higher R and R_w indices (0.0574 and 0.0714, respectively). The final difference Fourier synthesis showed maxima residuals of 0.4 e/Å^3.

Acknowledgements

We thank the Centro di Studi sulla Sintesi e la Struttura dei Metalli di Transizione nei Bassi Stati di Ossidazione (C.N.R. Milano) for financial support.

References

1 For a review see: B. Bosnich, in Asymmetric Catalysis, Nato ASI Series, Martinus Nijhoff, Boston, 1986; P. Pino and G. Consiglio, Pure Appl. Chem., 55 (1983) 1781; J.W. Apsimon and T. Lee Collier, Tetrahedron, 42 (1986) 5157; H.B. Kagan, in G. Wilkinson, F.G.A. Stone and E.W. Abel (Eds.), Comprehensive Organometallic Chemistry, Pergamon Press, London, 1982, vol. 8, p. 463.
2 J. Tsuji, Pure Appl. Chem., 54 (1982) 197; B.M. Trost and T.R. Verhoeven, in G. Wilkinson, F.G.A. Stone and E.W. Abel (Eds.), Comprehensive Organometallic Chemistry, Pergamon Press, London, 1982, vol. 8, p. 799; J. Tsuji, in Organic Synthesis with Palladium compounds, Springer Verlag, New York, 1980.
3 R.C. Larock, H. Song, S. Kim and R.A. Jacobson, J. Chem. Soc. Chem. Commun., (1987) 834; T. Hayashi, A. Yamamoto and Y. Ito, J. Organomet. Chem., 338 (1988) 261; J.P. Genet, S. Jugé, J. Ruiz Montes and J.M. Gaudin, J. Chem. Soc. Chem. Commun., (1988) 718; J. Hayashi, K. Kanehira, T. Hagihara and M. Kumada, J. Org. Chem., 53 (1988) 113, and refs therein.
4 E. Cesarotti, M. Grassi and L. Prati, J. Chem. Soc., Dalton Trans., (1989) 161.
5 E. Cesarotti, A. Chiesa, G. Ciani and A. Sironi, J. Organomet. Chem., 251 (1983) 79.
6 E. Cesarotti, L. Prati, G.Ciani, A. Sironi and C. White, J. Chem. Soc., Dalton Trans., (1987) 1149.
7 J. Sandstrom, in Dynamic NMR spectroscopy, Academic Press, New York, 1982; B.E. Mann, in Dynamic NMR spectroscopy in Inorganic and Organometallic Chemistry, Annual Report on NMR Spectroscopy, vol. 12, p. 263, 1989.
8 J. Jeener, B.H. Meiere, P. Bachmann and R.R. Ernest, J. Chem. Phys., 71 (1979) 4546; G. Bodenhausen and R.R. Ernst, J. Am. Chem. Soc., 104 (1982) 1304.
9 M. Grassi, B.E. Mann, B.T. Pickup and C.M. Spencer, J. Magn. Res., 69 (1986) 92 and refs. therein.
10 G.A. Morris and R.A. Freeman, J. Magn. Res., 29 (1978) 433.
11 H. Kurosawa and N. Asada, Organometallics, 2 (1983) 251; J.W. Faller, in Advances in Organomet. Chem., Academic Press, London, 1977, Vol. 16, p. 211.
12 H. Kessler, M. Gehrke and G. Griesinger, Angew. Chem. Int. Ed. Engl., 27 (1988) 490, and refs. therein.
13 R. Benn and H. Gunther, Angew. Chem. Int. Ed. Engl., 22 (1983) 350.
14 SDP Plus, Version 1.0, Enraf-Nonius, Delft, The Netherlands, 1980.
15 A.C.T. North, D.C. Phillips, F.S. Mathews, Acta Cryst. A, 24 (1968) 351.
16 International Tables for X-ray Crystallography, Vol. IV, Kynoch Press, Birmingham, 1974.